Nucleic Acids Research, 1993, Vol. 21, No. 6 1381–1387

In vitro selection of fast-hybridizing and effective antisense RNAs directed against the human immunodeficiency virus type 1

Karola Rittner, Christoph Burmester[1] and Georg Sczakiel*
Forschungsschwerpunkt Angewandte Tumorvirologie, Deutsches Krebsforschungszentrum, Im Neuenheimer Feld 242, D-6900 Heidelberg and [1]Max-Planck-Institut für Medizinische Forschung, Abteilung Biophysik, Jahnstraße 29, D-6900 Heidelberg, Germany

Received January 4, 1993; Revised and Accepted February 12, 1993

ABSTRACT

The rate of double strand formation between procaryotic antisense RNA and complementary RNA *in vitro* is known to correlate with the effectiveness of antisense RNA *in vivo*. In this work, an *in vitro* assay for determining the hybridization rates of a large number of antisense RNA species was developed. A set of HIV-1-directed antisense RNAs with the same 5′-end but successively shortened 3′-ends was produced by alkaline hydrolysis of a 150 nt HIV-1-directed antisense transcript. This mixture was used to determine hybridization rates for individual chain lengths with a complementary HIV-1-derived RNA *in vitro*. The second order binding rate constants of individual antisense RNA species differed by more than a factor of 100, although in some cases, slow-hybridizing and fast-hybridizing antisense RNAs differed by only two or three 3′-terminally-located nucleotides. The results indicated that there was not a trivial dependence of binding rates on the chain length of antisense RNAs. Further, the binding rate constants determined *in vitro* for individual antisense RNA species correlated with the extent of inhibition of HIV-1 replication *in vivo*.

INTRODUCTION

Antisense nucleic acid-mediated control of gene expression and viral replication plays an increasingly significant role *in vivo* and in tissue culture cells (for review see: 1–3). Relatively short synthetic and in many cases chemically modified antisense oligonucleotides have been applied successfully to living cells (reviewed in:4,5) as well as long antisense RNAs synthesized *in vitro* or, in most cases, expressed intracellularly from antisense genes (reviewed in: 6–8). Despite the great number of phenomenological descriptions of convincing biological effects obtained with antisense nucleic acids, unequivocal experimental evidence for the antisense principle has not been reported as frequently. In particular for eucaryotic antisense RNAs, systematic mechanistic analyses of double strand formation with target RNA *in vitro* and *in vivo* are lacking. In contrast to this, procaryotic antisense RNA-regulated examples have been studied in more detail. For the antisense RNA-regulated plasmid copy number in *E.coli* it has been shown that the kinetic behaviour of antisense RNA *in vitro* is in agreement with the effectiveness *in vivo* (9). For replication of plasmid R1, the kinetic situation for binding of antisense RNA to target RNA appears to reflect the antisense RNA-mediated control *in vivo* (10). Further, structural properties of individual antisense RNAs determine hybridization kinetics *in vitro* (11) and are linked with biological effects, e.g. plasmid copy numbers (reviewed in: 12,13). It is reasonable to assume that in principle these findings are also relevant for other antisense RNA-regulated or -inhibited systems, including eucaryotic ones (14). The biological systems in which most of the reported studies with antisense RNA have been conducted include the antisense RNA-mediated inhibition of the human immunodeficiency virus type 1 (HIV-1) replication (15–21). For this reason we have started to investigate kinetic properties *in vitro* of a HIV-1-directed antisense RNA (αY150) which was shown earlier to inhibit viral replication (Homann et al., manuscript in preparation). For a systematic analysis, individual binding rate constants of successively shortened antisense RNA species derived from αY150 were measured by a specific experimental approach developed in this work. The results showed a surprisingly high variation between second order binding rate constants ranging from $k < 5\times10^2$ $M^{-1}s^{-1}$ to $k > 1\times10^4$ $M^{-1}s^{-1}$ of subsets of antisense RNA, although chain lengths were similar. Fast- and slow-hybridizing antisense RNAs were tested for their antiviral activity in a transient HIV-1 replication assay. It was found that the second order binding rate constants correlated qualitatively with the extent of inhibition of HIV-1 replication.

The experimental strategy developed in this study to determine binding rate constants for a large number of different antisense RNA species contained in a pool of antisense RNAs is applicable for any sequence of interest and might support the systematic search for and the identification of kinetic parameters *in vitro*

* To whom correspondence should be addressed

which could serve as indicators for the effectiveness of antisense RNAs *in vivo*. For inhibition studies of HIV-1 replication the results might help in the identification of more potent antisense RNA species.

MATERIALS AND METHODS

Plasmids for *in vitro* synthesis of antisense RNAs and target RNA

The HIV-1-directed antisense RNAs were transcribed *in vitro* from plasmid pBS150 which contains two stretches of HIV-1 sequences (17 nts, pos.5807–5823; 93 nts, pos.5598–5506; ref. 22) in antisense orientientation with respect to a T7 promoter. The pBS150-derived antisense RNA αY150 contains additional polylinker sequences at its 5′-end (32 nts) and at its 3′-end (5 nts). The RNA strand containing complementary sequences to αY150 was transcribed *in vitro* from plasmid pRC-SR6 by using T7 polymerase. This sense-transcript contains a 562 nucleotide HIV-1 sequence (clone BH10, pos. 5366–5928; ref. 22) excised from plasmid pSR6 (23) and polylinker sequences at its 5′-end (74 nts) and at its 3′-end (6 nts).

In vitro transcription of RNA

T7 polymerase was used for *in vitro* transcription of αY150 and SR6 RNAs. Four mg of linearized template DNA (*XhoI* for αY150 and *NotI* for SR6) were incubated in a reaction mixture containing 18 mM Na_2HPO_4, 2 mM NaH_2PO_4, 5 mM NaCl, 20 mM dithiothreitol, 8 mM $MgCl_2$, 4 mM spermidine, and 1 mM nucleotidetriphosphates in a total volume of 200 µl. Reactions were started by adding 20 U of T7 polymerase and stopped after a 2 hrs incubation at 37°C by adding 300 µl 17 mM $MgSO_4$ and 20 U DNaseI. After a further incubation for 20 min at 37°C 750 µl 3 M sodium acetate were added and RNAs were precipitated with ethanol at 0°C. The pellet was dissolved in 10 mM Tris/HCL pH 8.0, 1 mM EDTA and the RNAs were further purified by gelfiltration (Sephadex G-50, Pharmacia). The recovery ranged between 40 µg and 50 µg RNA. The templates for the smaller αY150-derived antisense RNA species with chain lengths of 60, 67, 76, 82, 88, and 95 nucleotides were generated by PCR according to ref. 24 with an unique 5′-primer containing the T7 promoter sequence (5′ CCGGATCCAAGCTTTAATACGACTCACTATAGGG 3′) and 3′-primers (20mers) such that *in vitro* transcription of RNA terminates at the correct 3′-position. The PCR products were used for *in vitro* transcription without further subcloning.

^{32}P-labelling of RNAs

The 5′-ends of *in vitro* transcribed RNAs (10 ng) were ^{32}P-labelled by dephosphorylation with calf intestine phosphatase and subsequent rephosphorylation with 5 µCi of [γ-^{32}P]-ATP (10.0 mCi/ml, 6000 Ci/mmol) and polynucleotide kinase as described (25).

Alkaline hydrolysis of αY150-derived antisense RNA

For the production of a random mixture of successively shortened antisense RNAs a modification of an established protocol for alkaline hydrolysis was used (26). Briefly, 10 ng of 5′-end labelled αY150 RNA dissolved in 20 µl TE-buffer were added to 500 µl 500 mM $NaHCO_3$ and heated to 96°C for 10 minutes. Hydrolysis was stopped by chilling the reaction mixture and RNAs were desalted by gel filtration (Sephadex G-50, Pharmacia) with a buffer containing 10mM Tris/HCl pH8.0 and 1 mM EDTA. In order to make native and unique folding of RNA species possible which does not necessarily happen during the quick chilling on ice water the desalted mixture of RNAs was incubated at 75°C for 10 minutes and cooled down slowly to 37°C for renaturation.

Assay for selective identification of fast-hybridizing antisense RNAs—analysis of hybridization products

The stepwise experimental procedure is schematically shown in Figure 1. First, one ng of hydrolyzed 5′-labelled αY150 RNA corresponding to 2×10^{-14} moles of starting 5′-labelled αY150 RNA (1×10^{-9} M) was mixed with 500 ng unlabelled target RNA SR6 (2.2×10^{-12} moles, 1.1×10^{-7} M) at a final volume of 20 µl and at 37°C in a solution containing 100 mM NaCl, 20 mM Tris/HCl pH 7.4 and 10 mM $MgCl_2$. After certain time points of incubation, 3 ml aliquots were withdrawn and transferred into a precooled (0°C) Eppendorf tube containing 40 µl stop buffer (20 mM Tris/HCl pH 8.0, 10 mM EDTA, 0.5% SDS, 7 M urea, 0.04% bromphenolblue, 0.04% xylenecyanol). Educts and products of the hybridization reaction were separated on 1.2% agarose gels in 89 mM Tris–borate buffer pH 8.3 containing 1 mM EDTA. Agarose slices containing educts and products repectively were excised and RNAs were eluted by centrifugation of the frozen and thawed (–70°C/37°C) gel slizes. RNAs were precipitated with ethanol, redissolved with stop buffer (see above) and analyzed by electrophoresis under denaturing conditions in 10% polyacrylamide gels containing 7 M urea in 89 mM Tris-borate pH 8.3. Gels were fixed in an aqueous solution containing 10% methanol and 10% acetic acid, dried and exposed to X-ray film or to image plate analysis for further computer-supported quantitative analysis.

Determination of hybridization rates for individual antisense RNA species

For quantitative analysis of band intensities of dried polyacrylamide gels, a self-constructed image plate scanner (27) with a linear characteristic vs ^{32}P radioactivity was used. Gels were scanned with 37.5 µm×37.5 µm pixelsize. Each lane of the gel was analyzed individually. The data for each band were integrated along a direction perpendicular to the direction of migration. The resulting profiles of intensity against migration distance were displayed using a programme which allowed subtraction of background and integration of the individual peaks. Maximal values for each band were taken as a measure for the band intensities. For bands representing certain antisense RNA species at different time points of the hybridization reaction band intensities were plotted against the time axis and a curve for an exponential decay ($I=I_0\times e^{-kt}$) was fitted by non linear regression using the programme 'GRAFIT' (Erithacus Software, London, UK). The error range for k was derived from the fitting algorithmn as the standard deviation of k.

Computer-calculated RNA structures

The secondary structures of RNAs were calculated with the programme *Heidelberg Unix Sequence Analysis Resources (HUSAR)* which makes use of the secondary structure prediction algorithmn developed by Zuker and Stiegler (28).

HIV-1 inhibition studies

For measurements of antisense RNA-mediated inhibition of HIV-1 replication, *in vitro* synthesized RNAs (120 ng) and infectious proviral HIV-1 DNA (pNL4-3, 40 ng) respectively,

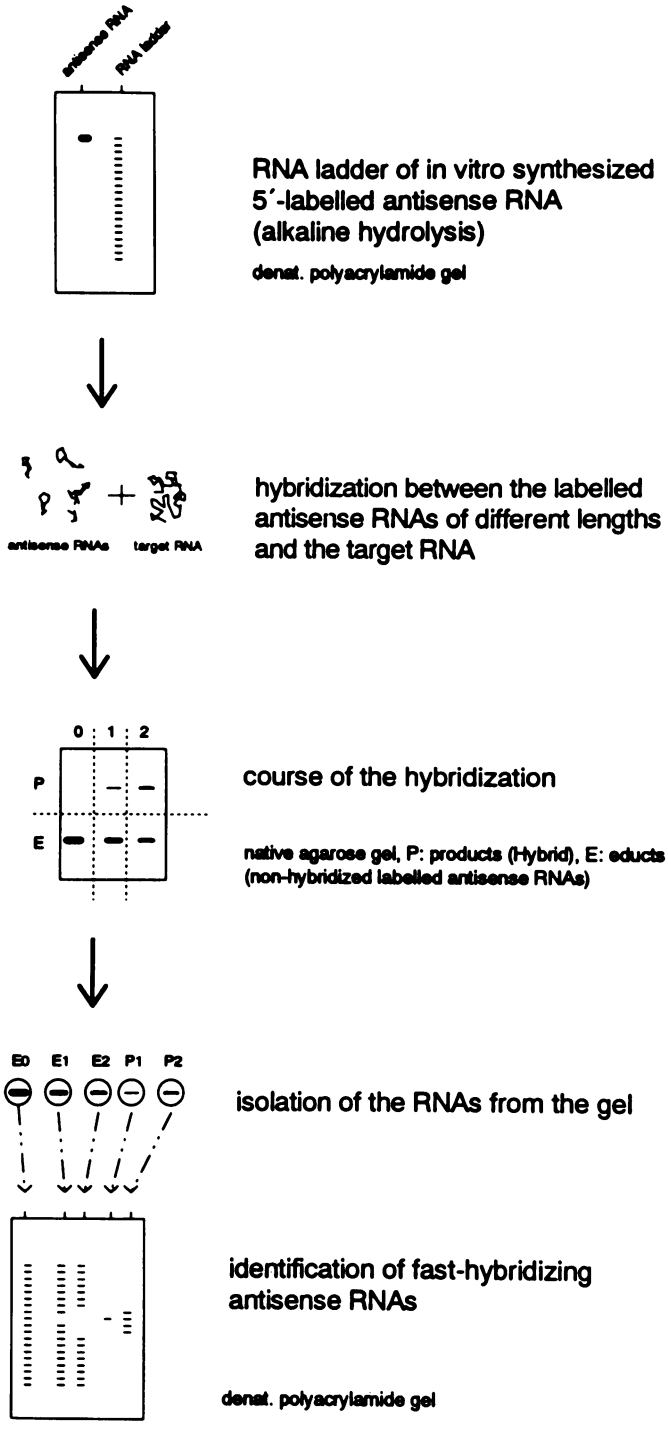

Figure 1. Schematic depiction of *in vitro* selection and identification of fast-hybridizing antisense RNAs.

were cotransfected by calciumphosphate co-precipitation (29) into human SW480 cells (30) which were grown semi-confluent in 48 well plates. One day after transfection 1×10^5 MT-4 cells were added and the final volume was adjusted to 1 ml. Virus replication was measured 4 days after transfection with dilutions of cell-free culture supernatants by a commercial HIV-1 antigen ELISA (Organon, Holland) as described in detail elsewhere (15). As a control *in vitro* synthesized CAT-coding RNA was used which had been shown before to have no effect on HIV-1 replication (23).

This assay leads to results similar to those obtained with an earlier described co-microinjection assay (15,23) except that the error range is significantly smaller for the latter assay.

Limited RNase cleavage of RNA

For RNase mapping, the 5'-ends of RNAs were ^{32}P-labelled by dephosphorylation with calf intestine phosphatase and subsequent rephosphorylation with [γ-^{32}P]-ATP and polynucleotide kinase as described (25). The cleavage reactions were performed in 100 mM NaCl, 20 mM Tris/HCl pH 7.4, 10 mM $MgCl_2$ with the following enzyme concentration: RNase T1, 10 U/ml (Boehringer, Mannheim). The reactions were stopped by adding the sample volume stop buffer (20 mM Tris/HCl pH 8.0, 10 mM EDTA, 0.5% SDS, 7 M urea) and chilling on ice. Cleavage products were separated on denaturing polyacrylamide gels (10%) buffered with 89 mM Tris–borate pH 8.3, 2.5 mM EDTA and 7 M urea.

RESULTS

Assay for identifying antisense RNAs with different hybridization rates

The antisense RNA used in this study (αY150) was directed against exons coding for Tat and Rev and was previously shown to be able to inhibit viral replication (unpublished) in an assay which was used earlier to measure inhibitory effects of *in vitro*-synthesized HIV-1-directed antisense RNAs (23). In order to systematically analyze possible variations in hybridization rates of a set of αY150-derived RNAs which differ in length and, most probably, also in structure we performed the assay which is schematically depicted in Figure 1. A ladder of successively shortened 5'-labelled αY150-derived antisense RNAs was produced by alkaline hydrolysis of 5'-end labelled αY150 RNA (see lane: 0' educts in Figure 2). The resulting mixture of antisense RNAs was incubated with a 110-fold molar excess of complementary unlabelled SR6 RNA in a physiological buffer at 37°C. This excess of SR6 RNA over ^{32}P-labelled antisense RNAs was chosen for several reasons: Firstly, it allowed the determination of rate constants according to pseudo first order kinetics. Under those conditions the hybridization rate is not dependent on the concentrations of ^{32}P-labelled antisense RNA species, i.e. differences in initial concentrations of antisense RNAs do not affect the determination of second order rate constants. Secondly, formation of a defined heteroduplex RNA was favoured versus other possible reactions of labelled antisense RNAs which were observed at equimolar concentrations of αY150 and SR6 RNA (Homann et al., unpublished). Lastly, competition among antisense RNAs for complementary RNA strands which could influence the selective determination of k values for individual antisense RNA species was excluded.

The course of the overall hybridization reaction was monitored by separating educts and products by agarosegel electrophoresis. The ^{32}P-labelled antisense RNAs which were equal to or smaller than 150 nts could be clearly distinguished on agarose gels from product bands, i.e. heteroduplex RNA consisting of one antisense RNA strand and a 562 nts complementary RNA. In order to select and identify individual antisense RNA species contained in early-appearing products of the overall reaction, i.e. fast-hybridizing antisense RNAs, educt bands and product bands were cut out of the agarose gel, RNAs were eluted and analyzed by polyacrylamidegel electrophoresis under denaturing conditions. We did not observe a dependence of elution efficiencies from

agarose gels on RNA lengths, however, the elution efficiencies measured for educts, i.e. single-stranded RNAs were significantly greater than those for the double-stranded products. Since the elution efficiency in neither case was dependent on the relative amounts of RNA contained in the eluted bands, the determination of k values was not affected.

Determination of rate constants for individual antisense RNA species

Presumably, many successive and perhaps easily reversible steps take place between antisense RNA and target RNA before duplex RNAs are formed completely. Since the melting points of the resulting long RNA double strands are high under physiological experimental conditions used in this work, the backward reaction is neglected in the analysis. Therefore, the simplified scheme for the overall hybridization reaction between antisense RNA species ($aRNA_i$) and sense RNA (sRNA) can be described as:

$$\alpha RNA_i + sRNA \rightarrow dsRNA$$

The initial rate of hybridization can be calculated as:

$$v_i = k_{2i} \times [\alpha RNA_i] \times [sRNA] \qquad \text{(eq. 1)}$$

Since the unlabelled sRNA is in large excess over αRNA and, hence, can be regarded as constant during the reaction, [sRNA] can be included in the rate constant k_{2i}:

$$v_i = k_{1i} \times [\alpha RNA_i] \text{ with } k_{1i} = k_{2i} \times [sRNA] \qquad \text{(eq. 2)}$$

This is the equation for a reaction of first order for which k_{1i} can be calculated from the time dependence of the binding of αRNA_i to sRNA:

$$[\alpha RNA_i]_t = [\alpha RNA_i]_0 \times e^{-k_{1i}t} \qquad \text{(eq. 3)}$$

and k_{1i} can be calculated from a computer fit to the data obtained. The value of k_{2i} can be calculated from the relationship: $k_{1i} = [sRNA] \times k_{2i}$

The band pattern of educts and products separated by electrophoresis with 10% polyacrylamide gels under denaturing conditions clearly demonstrates that disappearing educt bands, i.e. antisense RNA species, correspond to appearing product bands (Figure 2). Further, there are groups of fast-hybridizing antisense RNA species as well as visibly slow-hybridizing species. For example, fast-hybridizing antisense RNAs range in size between 65 and 78 nts and also occur at 57 nts, 97 nts and 110 nts.

Bands containing educts and products of typical hybridization reactions were quantified by using image plate detection and computer-based quantification as described in Materials and Methods. For a more detailed analysis we chose the size range of 57 to 99 where individual bands could be assigned and differences in hybridization rates were significant. The time-dependent change of educt- and product-signals derived from a representative gel analysis showed that educts in certain size ranges (e.g. 66 to 77 nts) hybridize significantly faster ($k \approx 1\times10^4\ M^{-1}s^{-1}$) than those RNA species from other size ranges (e.g. 58–63 or 80–84, Figure 3). For individual antisense RNA species rate constants for the hybridization reaction were calculated by using a fitted curve for the time-dependent decrease of educts (Figure 3). The value for k was calculated for the full length αY150 RNA on the basis of image plate analysis ($k = 1.17\times10^4\ M^{-1}s^{-1}$) and compared to values for k determined according to established protocols ($k = 1.30\times10^4\ M^{-1}s^{-1}$, ref. 31) or to densitometric analysis of band intensities with autoradiographs of polyacrylamide gels ($k = 1.56\times10^4\ M^{-1}s^{-1}$, data not shown). The k value determined by densitometric analysis of autoradiographs with dried polyacrylamidegels is somewhat greater which is due to the overestimation of differences of band intensities by this method. Since the hybridization rate constant for full length αY150 RNA which had been determined recently to $k = 1.30\times10^4 \pm 0.10\times10^4\ M^{-1}s^{-1}$ (32) is in agreement with the binding rate constant for αY150 RNA as determined in this work ($k = 1.17\times10^4\ [M^{-1}s^{-1}]$), we conclude that k values determined by the assay described here are valid.

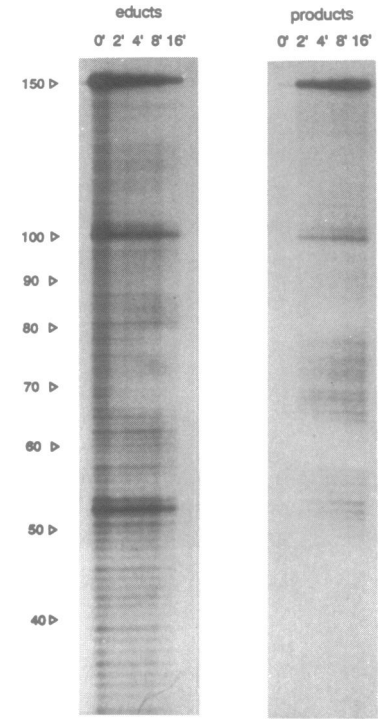

Figure 2. Experimental identification of fast-hybridizing αY150-derived antisense RNAs by electrophoresis with 10% polyacrylamide gels under denaturing conditions according to the scheme shown in Figure 1. Samples were withdrawn from the hybridization reaction mixture at the time points indicated.

Binding rate constants and RNA structures

The binding rate constants measured in this work for successively shortened antisense RNAs were compared with the total free energies, the free energy per length, and the computer-predicted secondary structures for each individual molecule (Figure 4). These data do not suggest a correlation between k and any of the structural parameters. The differences between the free energies for the slow-hybridizing antisense RNA species, i.e. −0.29 to −0.25 kcal/nt for the 60mer, 82mer and 95mer and the corresponding parameters for the fast-hybridizing species do not seem to be significant. However, the sensitivity of individual shortened RNAs against RNaseT1 indicates that small k values might correlate with a reduced RNase sensitivity except for the 82mer which will be discussed later (Figure 4A).

Previously performed extensive experimental structure analysis of αY150 did not support the predicted secondary structure shown in Figure 4B (Homann et al., manuscript in preparation). In general, mapping of a given RNA molecule by limited cleavage experiments with structure-specific RNases does not enable one

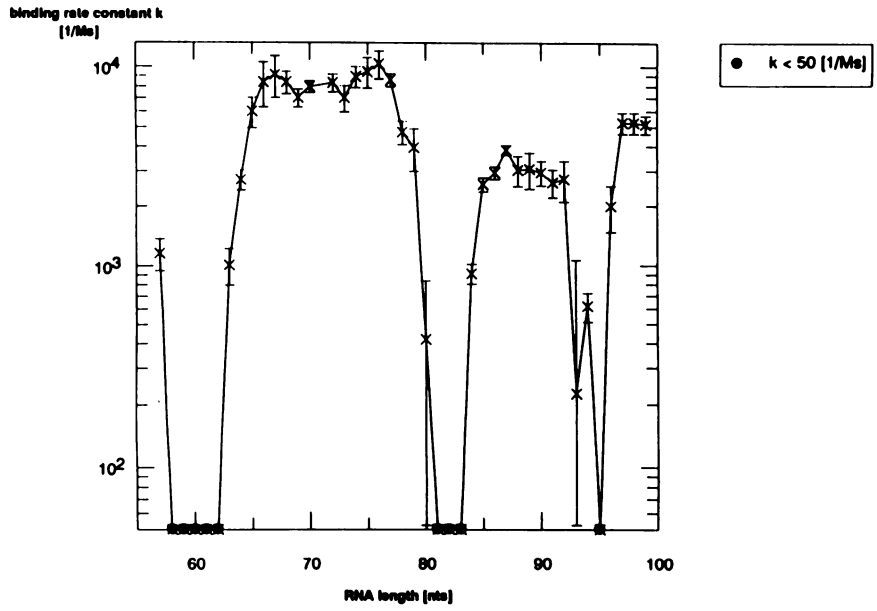

Figure 3. Second order rate constants (k) of the hybridization reaction between αY150-derived antisense RNA species ranging in lengths between 57 and 99 nucleotides (x-axis) and a transcript containing 562 nts of complementary sequence.

to derive an exact model. However, RNase cleavage patterns may indicate similarities or differences between given RNA molecules. The results of RNaseT1 cleavage reactions with the 60mer, 67mer, 76mer, 82mer, 88mer, 95mer, and αY150 respectively, indicate differences in the 3′ portion of the slow-hybridizing 95mer versus the 76mer (fast), 88mer (fast) and αY150 (fast) which also seem to exist versus the fast 67mer (Figure 5). The 60mer, however, lacks this sequence and the 82mer (slow) seems to show the double band labeled in Figure 5, even though significantly weaker than the fast-hybridizing species. Thus, one might conclude that the local structures of the sequences in the range of positions 60 to 70 have an effect on the binding rate constants in vitro.

Correlation between binding rate constants and the extent of inhibition *in vivo*

In order to investigate whether the binding rate constants were correlated with the biological effectiveness, we co-transfected *in vitro* synthesized fast- and slow-hybridizing antisense RNA species with infectious proviral HIV-1 DNA into human cells and measured the resulting production of HIV-1 (Figure 6). Three out of three fast-hybridizing antisense RNAs (67mer, 76mer and 88mer) led to strong inhibition of HIV-1 replication and two out of three slow-hybridizing antisense RNAs (60mer and 95mer) led to a reduced or no significant inhibition respectively. These results indicate that there is a qualitative correlation between the k values and the inhibitory effectiveness for the αY150-derived antisense RNAs. Possible reasons for the strong inhibition mediated by the 'slow' 82mer will be discussed later. Future experiments should investigate whether there is also a quantitative correlation between both parameters. It is somewhat surprising that the extent of inhibition *in vivo* mediated by the full length antisense RNA αY150 is smaller than that of the fast-hybridizing 67mer, 76mer and 88mer respectively. However, we cannot exclude that the significant difference in chain length between

A

RNA length nts	ΔG kcal	ΔG per length	k_2 1/Ms	sensitivity against RNase T1
150	-43,7	-0,29	$1,5 \times 10^4$	high
95	-27,2	-0,27	≤ 50	low
88	-21,5	-0,24	2×10^3	high
82	-20,6	-0,25	≤ 50	high
76	-17,8	-0,23	9×10^3	high
67	-15,8	-0,24	$8,5 \times 10^3$	high
60	-15,8	-0,26	≤ 50	medium

B

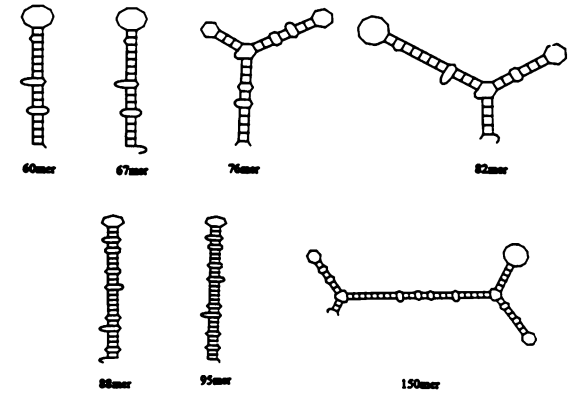

Figure 4. A) Relationship between k, ΔG, ΔG per length, computer-predicted secondary structures, and sensitivity against RNaseT1 of selected fast- and slow-hybridizing antisense RNAs derived from αY150. B) Mapping of RNA strcutures by limited cleavage reactions with RNaseT1.

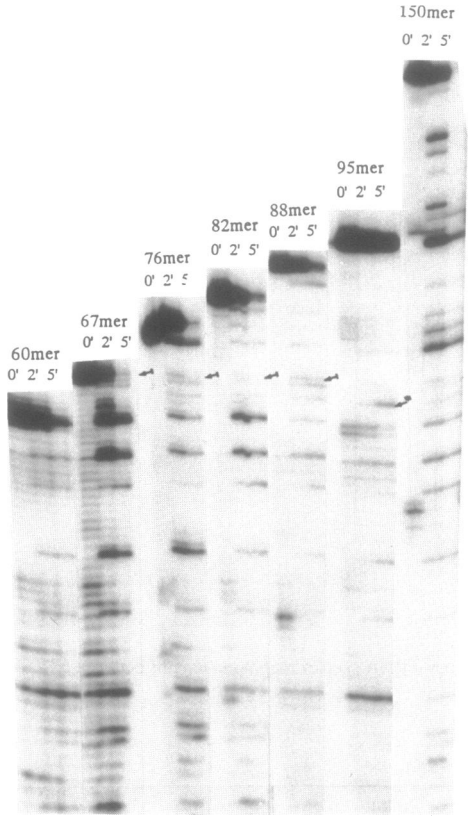

Figure 5. RNaseT1 mapping of αY150 and αY150-derived shortened species. A structural difference in the 5′ portion of the RNAs is indicated by a differentially appearing double band (pos. 66 and 67) and one single band (pos. 64) labelled by arrows. The double band is clearly visible for all fast-hybridizing RNAs, i.e. the 67mer, 76mer, 88mer and αY150 repectively. To a minor extent the RNaseT1-produced double band is also visible for the slow-hybridizing 82mer. Position 64 of the slow-hybridizing 95mer seems to be particularly sensitive to RNaseT1.

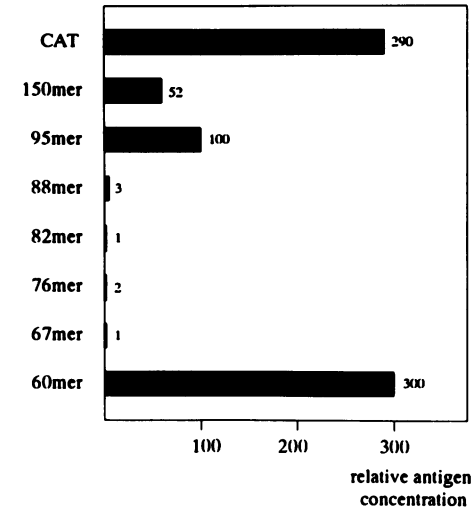

Figure 6. Replication of HIV-1 in the presence of selected fast- and slow-hybridizing antisense RNAs derived from αY150. The bars indicate the mean of two series of five individual transfection experiments each.

αY150 on the one hand and the 67mer, 76mer, and 88 mer on the other hand contributes to this observation.

DISCUSSION

In this work an *in vitro* assay is described in which individual binding rate constants for a series of antisense RNAs to target RNA could be determined in parallel. Measurements with a set of HIV-1-directed antisense RNAs showed that subsets of antisense RNAs with the same 5′-end but differing in their 3′-ends differ in their hybridization rates with the complementary RNA. A simple length-dependent change of k values was not observed but, groups of fast-hybridizing antisense RNA species with k values in the range of 1×10^4 [$M^{-1}s^{-1}$] (66−77, Figure 3) and 3×10^3 [$M^{-1}s^{-1}$] (85−92, Figure 3) on the one hand and slow-hybridizing ones ($k < 5\times10^2$ [$M^{-1}s^{-1}$] Figure 3) on the other hand were detected.

The hybridization rate for αY150 ($k = 1.3\times10^4$ M^1s^{-1}) is smaller by more than one order of magnitude when compared to naturally occuring antisense RNAs with similar lengths (ca $3-10\times10^5$ [$M^{-1}s^{-1}$], summarized in ref. 32). The difference between the binding rate constants determined for fast-hybridizing antisense RNAs in this work and the binding rates for naturally occuring antisense RNAs indicate that further enhancement of the rate of double strand formation between HIV-1-directed antisense RNA and target RNA might be achievable. Thus, kinetic analyses of antisense RNA target RNA interactions could be specifically meaningful for further systematic improvements of the antiviral effectiveness of HIV-1-directed antisense RNAs and might be valuable in general for the design of effective antisense constructs.

The transitions from slow-hybridizing to fast-hybridizing antisense RNA species (e.g. pos. 62/65 in Figures 1 and 2) and vice versa (e.g. pos. 78/81 in Figure 2) were found to happen in a small size range. Thus, the question arises whether major structural changes at these chain lengths are linked with the change of k values. For example it is conceivable that the structures of antisense RNAs ranging in length between 66 and 77 share common properties in the sense of similar kinetic characteristics concerning double strand formation, whereas antisense RNAs between 85 and 92 nts in length differ significantly in this respect. For this reason we calculated the k values for all antisense RNAs ranging from 57 to 99 nucleotides on the basis of educt-decrease and compared these with computer-predicted secondary structures calculated according to (28) and corresponding stability parameters for the folded molecules (Figure 4). However, the results do not indicate a correlation between k values and the predicted structural parameters or corresponding ΔG values respectively. Since computer-aided secondary structure prediction is still not very reliable, we started to compare structures of fast-hybridizing antisense RNAs with slow-hybridizing antisense RNAs experimentally. Limited RNAseT1 cleavage reactions with the antisense RNA species listed in Figure 4A indicated that there was a structural difference in the 3′ portion of the slow-hybridizing 95mer versus the other antisense RNAs (Figure 5). For the small and slow 60mer but not the 95mer we cannot exclude that the size of the antisense sequence is too small for efficient inhibition *in vivo*. One exception seems to be the slow-hybridizing 82mer which led to significant inhibition of HIV-1 replication (Figure 6). In contrast to this, there is only minor experimental evidence for structural differences between the slow 82mer and the fast-hybridizing species which might explain the strong *in vivo* effects of the 82mer (Figure 5) although the binding rate constant *in vitro* was small.

However, it is known and it can be seen in Figure 5 that *in vitro* transcription of RNA leads to considerable amounts of shortened and extended transcripts (at least up to three nucleotides). In particular, preparations of the 82mer also contain fast-hybridizing species. For example, the 79mer and 80mer as well as the 84mer and 85mer contained in 82mer preparations might be sufficient to inhibit HIV-1 replication. The experimental conditions for determining HIV-1 replication were chosen such that a further comparison of the antiviral effectiveness of the inhibitory antisense RNA species (82mer versus 67mer, 76mer, and 88mer) was not possible.

Future work should be focused on two questions: What is the molecular (structural) basis for the relatively high k values of fast-hybridizing antisense RNAs versus the k values for slow-hybridizing antisense RNAs? Are k values for individual antisense RNAs correlated with the inhibitory effectiveness in living cells? Quantitative results could be achived in the case of HIV-1 by use of the microinjection technique (33).

In general, it is not clear whether the experimental conditions for studying RNA/RNA interactions *in vitro*, even though performed at physiological ion strength and at 37°C reflect the situation *in vivo*. For example in living cells, factors which bind to RNA might influence the free energy of individual molecules or the activation energy of the binding reaction, the structures, and the interactions between antisense RNA and target RNA respectively (34,35). However, for naturally occuring antisense RNA-regulated and well-studied procaryotic systems it has been shown that kinetic analyses support the understanding of the function of antisense RNA. The same view might be true for the eucaryotic example described in this work.

The *in vitro* selection of fast-hybridizing antisense RNAs extends those *in vitro* systems by which a given pool of therapeutically or biologically interesting and/or relevant macromolecules such as polypeptides or nucleic acids can be selected for desired properties. In this view, the approach decribed here might be improved if it was possible to increase the number of individual species in the starting pool and to select with more than one selection step.

ACKNOWLEDGEMENTS

We thank H.zur Hausen for continuous support, R.S.Goody for stimulating discussion and for critically reading this manuscript, R.Schröder for helpful advices with image plate analysis and M.Homann for plasmid pBS150.

REFERENCES

1. Simons,R.W. (1988) *Gene*, **72**, 35–44.
2. Weintraub,H.B. (1990) *Sci. Am.*, **262**, 34–40.
3. Hélène,C., and Toulmé,J.J. (1990) *Biochem. Biophys. Acta*, **1049**, 99–125.
4. Ts'O,P.O.P., Miller,P.S., Aurelian,L., Murakami,A., Agris,C., Blake,K.R., Lin,S.-B., Lee,B.L., and Smith,C.C. (1990) *Ann. NY Acad. Sci.*, **507**, 220–241.
5. Stein,C.A., and Cohen,J. (1988) *Cancer Res.*, **48**, 2659–2668.
6. Walder,J. (1988) *Genes Dev.*, **2**, 502–504.
7. Takayama,K.M. and Inouye,M. (1990) *Crit. Rev. Biochem. Mol. Biol.*, **25**, 155–184.
8. Green,P.J., Pines,O., and Inouye,M. (1986) *Ann. Rev. Biochem.*, **55**, 569–597.
9. Tomizawa,J.-i, and Som,T. (1984) *Cell*, **38**, 871–878.
10. Nordström,K., Wagner,E.G.H., Persson,C., Blomberg,P., and Öhman,M. (1988) *Gene*, **72**, 237–240.
11. Persson,C., Wagner,E.G.H., and Nordström,K., (1990) *EMBO J.*, **9**, 3767–3775.
12. Novick,R.P. (1987) *Microbiol. Rev.*, **51**, 381–395.
13. Polsky,B. (1988) *Cell*, **55**, 929–932.
14. Inouye,M. (1988) *Gene*, **72**, 25–34.
15. Sczakiel,G., Pawlita,M., and Kleinheinz,A. (1990) *Biochem. Biophys. Res. Comm.*, **169**, 643–651.
16. Rhodes,A., and James,W. (1990) *J. Gen. Virol.*, **71**, 1965–1974.
17. Rhodes,A., and James,W. (1990) *AIDS*, **5**, 145–151.
18. Renneisen,K., Leserman,L., Matthes,E., Schröder,H.C., Müller,W.E.G. (1990) *J. Biol. Chem.*, **265**, 16337–16342.
19. Sczakiel,G, and Pawlita,M. (1991) *J. Virol.*, **65**, 468–472.
20. Sczakiel,G, Oppenländer,M., Rittner,K., and Pawlita,M. (1992) *J. Virol.*, **66**, 5576–5581.
21. Lo,K.M.S., Biasolo,M.A., Dehni,G., Palú,G., and Haseltine,W.A. (1992) *Virology*, **190**, 176–183.
22. Ratner,L., Haseltine,W., Patarca,R., Livak,K.J., Starcich,B., Josephs,S.F., Doran,E.R., Rafalski,J.A., Whitehorn,E.A., Baumeister,K., Ivanoff,L., Petteway Jr.,S.R., Pearson,M.L., Lautenberger,J.A., Papas,T.S., Ghrayeb,J., Chang,N.T., Gallo,R.C., and Wong-Staal,F. (1985) *Nature (London)*, **313**, 277–283.
23. Rittner,K., and Sczakiel,G. (1991) *Nucl. Acids Res.*, **19**, 1421–1426.
24. Schwartz,S., Felber,B.K., Benko,D.M., Fenyö,E.-M., and Pavlakis,G. (1990) *J. Virol.* **64**, 2519–2529.
25. Maniatis,T., Fritsch,E.F., and Sambrook,J. (1982) *Molecular Cloning: A laboratory manual*. Cold Spring Harbour Laboratory Press, Cold Spring Harbour, N.Y.
26. Beijer,B., Sulston,I., Sproat,B.S., Rider,P., Lamond,A.I., and Neuner,P. (1990) *Nucl. Acids Res.*, **18**, 5143–5151.
27. Burmester,C., and Schröder,R.R. (1992) *Proc. of the European Congress of Electronmicroscopy*, Eurem 92, Granada, Electronmicroscopy, Vol.1, pp. 95–96.
28. Zuker,M., and Stiegler,P. (1981) *Nucl. Acids Res.*, **9**, 133–148.
29. Chen,C., and Okayama,H. (1987) *Mol. Cell. Biol.*, **7**, 2745–2752.
30. Leibovitz,A., Stinson,J.C., McCombs III,W.B., McCoy,C.E., Mazur,K.C., and Mabry,N.D. (1976) *Cancer Res.* **36**, 4562–4569.
31. Persson,C., Wagner,E.G.H., and Nordström,K., (1988) *EMBO J.*, **7**, 3279–3288.
32. Sczakiel,G., Pawlita,M., Rittner,K., and Homann,M. (1992) *Ann. NY Acad. Sci.*, **660**, 268–271.
33. Sczakiel,G., Oelze,I. & Rittner,K. (1993) In: Bach, P., Reynolds,C.H., Clark,J.M., Poole, P. & Mottley, J. (eds.): *Biotechnology Applications of Microinjection, Microscopic Imaging and Fluorescence*, Plenum Press, London, pp.1–10.
34. Dreyfuss,G. (1986) *Ann. Rev. Cell. Biol.*, **2**, 459–498.
35. Munroe,S.H., and Dong,X. (1992) *Proc. Natl. Acad. Sci. USA*, **89**, 895–899.